

Two-frequency amplification in a semiconductor taperedamplifier for cold atom experiments

Zhi-Xin Meng(孟至欣), Yu-Hang Li(李宇航), Yan-Ying Feng(冯焱颖)

Citation: Chin. Phys. B . 2018, 27(9): 094201. **doi:** 10.1088/1674-1056/27/9/094201

Journal homepage: http://cpb.iphy.ac.cn; http://iopscience.iop.org/cpb

What follows is a list of articles you may be interested in

Tuning the velocity and flux of a low-velocity intense source of cold atomic beam

Shu Chen(陈姝), Ying-Ying Li(李营营), Xue-Shu Yan(颜学术), Hong-Bo Xue(薛洪波), Yan-Ying Feng(冯焱颖)

Chin. Phys. B . 2017, 26(11): 113703. **doi:** 10.1088/1674-1056/26/11/113703

Quantum feedback cooling of two trapped ions

Shuo Zhang(张硕), Wei Wu(吴伟), Chun-Wang Wu(吴春旺), Feng-Guang Li(李风光), Tan Li(李坦), Xiang Wang(汪翔), Wan-Su Bao(鲍皖苏)

Chin. Phys. B . 2017, 26(7): 074205. **doi:** 10.1088/1674-1056/26/7/074205

Spectral broadening induced by intense ultra-short pulse in 4H-SiC crystals

Chun-hua Xu(徐春华), Teng-fei Yan(闫腾飞), Gang Wang(王刚), Wen-jun Wang(王文军), Jing-kui Liang(梁敬魁), Xiao-long Chen(陈小龙)

Chin. Phys. B . 2016, 25(6): 064206. **doi:** 10.1088/1674-1056/25/6/064206

Off-resonant double-resonance optical-pumping spectra and their application in a multiphoton cesium magneto-optical trap

Yang Bao-Dong, He Jun, Wang Jun-Min

Chin. Phys. B . 2014, 23(5): 054205. **doi:** 10.1088/1674-1056/23/5/054205

Physical origin of observed nonlinearities in Poly (1-naphthyl methacrylate)：Using a single transistor–transistor logic modulated laser beam

Qusay M. A. Hassan, Hussain A. Badran, Alaa Y. AL-Ahmad, Chassib A. Emshary

Chin. Phys. B . 2013, 22(11): 114209. **doi:** 10.1088/1674-1056/22/11/114209

Two-frequency amplification in a semiconductor tapered amplifier for cold atom experiments*

Zhi-Xin Meng(孟至欣), Yu-Hang Li(李宇航), and Yan-Ying Feng(冯焱颖)†

State Key Laboratory of Precision Measurement Technology and Instruments, Department of Precision Instruments, Tsinghua University, Beijing 100084, *China*

(Received 26 June 2018; revised manuscript received 11 July 2018; published online 28 August 2018)

Simultaneous two-frequency amplification is highly desirable in cold atom experiments. The nonlinear response would appear in the two-frequency amplification with a semiconductor tapered amplifier (TA) and has a direct influence on the experimental result. We investigated in detail the effects of frequency difference, total power, and power ratio of two seeding lasers on the output components based on a simplified theoretical model. The simulation results showed that the multiple sideband generation in the amplifier due to self-phase and amplitude modulation could be suppressed and the TA tended to linearly amplify the power ratio between two-frequency components, when the two seeding lasers had a large frequency difference. This was verified experimentally in the output power ratio measurement via a calibrated Fabry–Perot interferometer method with a good linearity and an uncertainty of 1%. We also discussed the consequences of power ratio responses in the amplification in light of cold atom experiments, especially in the ac Stark shift related phase error of Raman-type atom interferometers (AIs). It was shown that the fluctuation of intensity ratio of Raman beams may induce significant systematic errors for an AI gyroscope.

Keywords: two-frequency amplification, self-phase modulation, laser cooling, atom interferometry

PACS: 42.60.Lh, 42.65.–k, 37.25.+k **DOI:** 10.1088/1674-1056/27/9/094201

1. Introduction

Simultaneous injection of two continuous wave (CW) lasers into a semiconductor tapered amplifier (TA) has become an efficient approach to obtain a high power two-frequency laser source,[1,2] and could find wide applications in many fields, such as laser cooling of atoms and molecules,[3–9] Raman optics for atom interferometers,[10] coherent population trapping (CPT) clocks,[11] and precision spectroscopy.[12–14] For a light pulsed atom interferometer, two-frequency optical amplification in a semiconductor TA, as a simple and cost-effective method, can be used to prepare a matter-wave source of alkali atoms via laser cooling where high power two-frequency components are required for optical pumping and cooling, or to generate Raman lasers for coherently manipulating a matter wave packet in a Raman-type atom interferometer.[10] In these optical systems, the fluctuation of power ratio between two-frequency components after a TA has a significant influence on the preparation efficiency of cold atoms or the phase of a Raman-type atom interferometer induced by the differential Raman light shift, which may deteriorate the ultimate level of performance in terms of accuracy as an inertial sensor.[15–25]

Early studies on semiconductor laser amplifiers showed that gain-saturation-induced nonlinearity could lead to a shape distortion and spectral broadening of optical pulses as a result of the self-phase modulation. Agrawal *et al.* obtained simplified equations governing the dynamics of the amplification process in the approximation that the optical pulse width was much larger than the intraband relaxation time.[26] Ferrari *et al.* experimentally studied the two-frequency CW components injection amplification in a semiconductor tapered amplifier, and observed significant additional frequency sidebands due to the nonlinearities in the TA for frequency differences less than 2 GHz.[27] The power of these additional sidebands could be decreased by operating the TA in a less saturated, and thus more linear regime. Luo *et al.* utilized the heterodyne frequency-beat measurement to analyze multiple sideband generation for two-frequency components injected into a TA under diverse experimental parameters such as frequency difference, injection laser power, and TA driving current.[28] The multiple sideband generation with a small frequency difference can show significant effects on the number of trapped atoms in laser cooling potassium 41 with hyperfine splitting of 245 MHz. Lévèque *et al.* reported a Raman laser scheme based on the amplification of two frequency lasers in a semiconductor TA and evaluated the phase noise arising from the amplification process and its impact on the performances of an atom interferometer.[29] It demonstrated that the amplification process did not induce significant phase noise or degradation of the performances of the interferometer. However, the frequency-dependent amplification in the TA may induce a change of the power ratio between two Raman lasers after the amplification and thus a change of the differential light shift,[30] which would lead to a bias in the gravity

*Project supported by the National Natural Science Foundation of China (Grant No. 61473166).

†Corresponding author. E-mail: yyfeng@tsinghua.edu.cn

© 2018 Chinese Physical Society and IOP Publishing Ltd

measurement in a Raman-type atom gravimeter and could not be compensated even by the k-reversal technique.[31]

In this paper, we investigate, both numerically and experimentally, the amplification of two CW lasers in the semiconductor TA. The simulation results show that the multiple sideband generation was influenced by the frequency difference, the total power, and power ratio of the seeding lasers. Experimental measurements using a calibrated Fabry–Perot interferometer (FPI) method agree well with the simulation results. Finally, we discuss the consequences of the amplification process on cold atom experiments, especially the effect of power ratio fluctuation on an atom interferometer gyroscope.

2. Theoretical model

The physical model for two-frequency laser amplification in a semiconductor amplifier was given by Agrawal,[26] describing the relevant self-phase modulation (SPM) and spectral broadening of optical pulses. This model can be simplified provided that the pulse width is much larger than the intraband relaxation time (typically 0.1 ps), which governs the dynamics of the induced polarization. The evolution of the laser inside a TA can be described as

$$\frac{\partial P}{\partial z} = (g - \alpha_{\text{int}})P, \tag{1}$$

$$\frac{\partial \phi}{\partial z} = -\frac{1}{2}\alpha g, \tag{2}$$

$$\frac{\partial g}{\partial \tau} = \frac{g_0 - g}{\tau_{\text{c}}} - \frac{gP}{E_{\text{sat}}(1+\mu z)}, \tag{3}$$

where τ is the reduced time measured in a reference frame moving with the light, $P(\tau,z)$, $\phi(\tau,z)$, and $g(\tau,z)$ are the power, the phase, and the gain, respectively. For other symbols, g_0 stands for the small signal gain, α_{int} for the internal loss which can be set as 0 if $\alpha_{\text{int}} \ll g$, α for the linewidth enhancement factor, τ_{c} for the carrier lifetime in the semiconductor, E_{sat} for the saturation energy of the amplifier, and μ for the amplifier splay factor. Equation (2) shows that a time-dependent gain would lead to a phase modulation. However, this can be neglected for CW lasers concerned in this work. In addition, all losses and dispersion effects can be neglected in our situation, and thus the above equations can be simplified as

$$\frac{\partial P}{\partial z} = gP, \tag{4}$$

$$\frac{\partial g}{\partial \tau} = \frac{g_0 - g}{\tau_{\text{c}}} - \frac{gP}{E_{\text{sat}}(1+\mu z)}. \tag{5}$$

When two lasers with a frequency difference of $\delta \equiv \nu_1 - \nu_2$ are injected into a TA, the electric field input is given by

$$E(t, z=0) = E_1 \exp[-\mathrm{i}(2\pi\nu_1 t - \phi_1)] + E_2 \exp[-\mathrm{i}(2\pi\nu_2 t - \phi_2)]. \tag{6}$$

Thus, the power of the beat note is given by

$$P(t, z=0) = P_0[1 + m\cos(2\pi\delta t + \phi)], \tag{7}$$

where $P_0 = E_1^2 + E_2^2$, $m = 2E_1E_2/(E_1^2 + E_2^2)$, and $\phi = \phi_1 - \phi_2$. By using the finite-difference method, equations (4) and (5) can be written as

$$\int_0^z \frac{\mathrm{d}P}{\mathrm{d}z}\mathrm{d}z = \int_0^z g_i P_{i-1}\mathrm{d}z, \tag{8}$$

$$\frac{g_i - g_{i-1}}{\Delta\tau} = \frac{g_0 - g_i}{\tau_{\text{c}}} - \frac{g_i P_{i-1}}{E_{\text{sat}}(1+\mu z)}. \tag{9}$$

The amplification of two CW lasers can be simulated by iterations of Eqs. (8) and (9), and the Fourier transform of $P(t,z)$ would give the beat signals between different orders of sidebands at the TA output, instead of the sidebands themselves. These beat signal frequencies will be denoted as $f_m = m\delta$, $m = 1, 2, 3, ..., p$, hereafter. Neglecting higher order beat signals, i.e., $m > 4$, the power of the beat signal at the TA output can be given by

$$\begin{aligned} &P(t, z = z_0) \\ &= P_0'[1 + a\cos(2\pi\cdot\delta t + \phi_1) + b\cos(2\pi\cdot 2\delta t + \phi_2) \\ &\quad + c\cos(2\pi\cdot 3\delta t + \phi_3) + d\cos(2\pi\cdot 4\delta t + \phi_4)], \end{aligned} \tag{10}$$

where z_0 is the length of tapered area, P_0' is the average output power, and a, b, c, and d are the relative powers for the beat signal with a frequency of f_m, $m = 1, 2, 3$, and 4, respectively.

3. Numerical simulations

In the numerical simulations, the parameters of TA was assumed to be $g_0 = 23731\ \text{m}^{-1}$, and $E_{\text{sat}} = 12$ pJ. The input power for each of the two lasers is 20 mW, and the frequency difference is 10 MHz. Figure 1 shows the Fourier transform of $P(t,z)$ at the output of the TA. High-order beat signals (2δ, 3δ, and 4δ) due to nonlinear process can be observed.

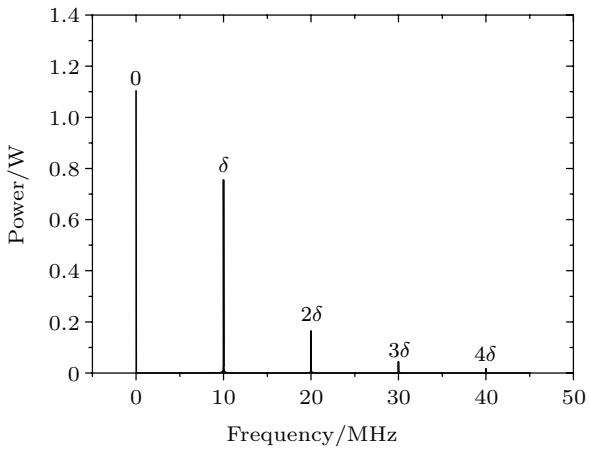


Fig. 1. (color online) Fourier transform of the TA output power $P(t,z)$. The input power for each of the two lasers is 20 mW, and the frequency difference is 10 MHz. The simulation parameters of TA are $g_0 = 23731\ \text{m}^{-1}$ and $E_{\text{sat}} = 12$ pJ.

First, we would like to study the effects of the total input power on relative powers when the total power changed from 5 mW to 50 mW (with identical power of the two input lasers) and the frequency difference of $\delta = 10$ MHz. From Fig. 2, it can be seen that the relative powers of b, c, and d increase with the total input laser power. For example, the relative power of 4δ increases from -36 dB to -17 dB when the total power increases from 5 mW to 50 mW. This can be explained by the fact that the input lasers gradually saturates the TA with the increasing power, and thus showing the nonlinear power amplification characteristics. Therefore, one can suppress multiple sideband generation by operating the TA in the range of lower injection laser power, i.e., a less saturated and more linear regime.

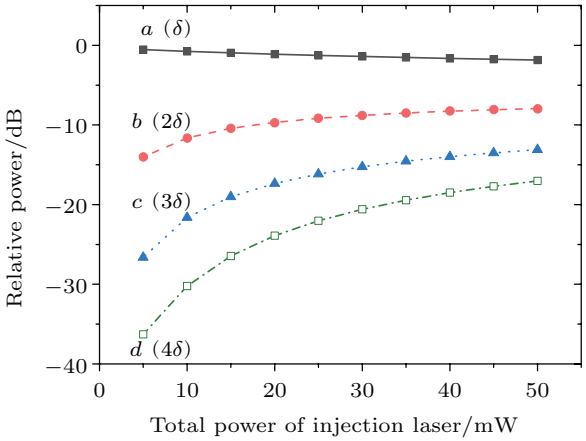


Fig. 2. (color online) Relative powers of the beat signals for different total input power. The power ratio of the two input lasers is 1:1, and the frequency difference $\delta = 10$ MHz. Other simulation parameters are the same with those in Fig. 1.

The multiple sideband generation originally comes from the wave mixing, and the power ratio of two-frequency components can influence the power distribution among different side-bands.[28] Figure 3 shows that the relative powers of the beat signals reach their maximum values when the input lasers have identical power.

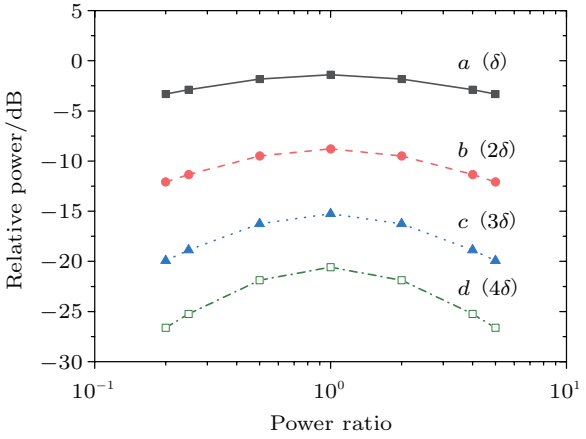


Fig. 3. (color online) Relative powers of the beat signals for different input power ratios. The frequency difference is $\delta = 10$ MHz and the total input power is 30 mW.

The effect of the frequency difference between the two input lasers on the beat signal has also been studied, and is shown in Fig. 4, in which the total injection power of 40 mW is assumed, with identical power of the two input lasers. It can be seen that the relative powers of the beat signals (a, b, c, and d) have no obvious changes when the frequency difference is low enough, i.e., below 500 MHz, 30 MHz, and 200 MHz for b, c, and d, respectively. When the frequency difference becomes higher, the relative power drops greatly. This can be ascribed to the finite carrier recovery time (300 ps here in the simulation) in the TA.[32] These simulation results mean that the multiple sideband generation in the TA can be extremely large when the frequency difference is small (e.g., a few MHz) and that it can only be neglected when the frequency difference is large enough (e.g., its reciprocal is comparable with the recovery time of the TA). This observation agrees well with experimental demonstrations in Refs. [27] and [28].

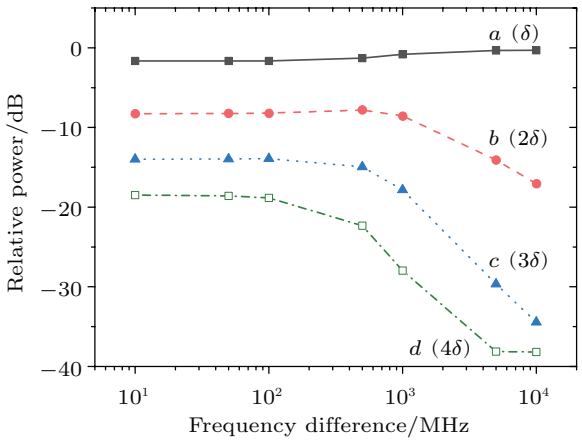


Fig. 4. (color online) Relative powers of the beat signals for different frequency differences δ. Other simulation parameters are the same with those in Fig. 1.

As indicated in Fig. 4, multiple sidebands generation can be neglected and output beams of the TA consist essentially of the frequency components, ν_1 and ν_2, when the frequency difference is large enough (e.g., above 1 GHz). Figure 5 agrees with this result, which shows that the output power ratio changes almost linearly with that of the input. Here, the data points are numerical simulation results and the straight lines are the corresponding linear fittings. It can be observed that the power amplification is almost linear for frequency difference higher than 2 GHz. However, the slope for the 1 GHz (i.e., 1.16) slightly deviates from 1. This can be explained by the amplification of the 2nd order sideband for the frequency difference of 1 GHz, since the 2δ component in the beat signal in Fig. 4 is also extremely large. In contrast, the 2δ component is negligibly small for other cases.

In the cold atom experiment involving laser cooling atoms of alkali metal, two-frequency amplification can be used for generating optical pumping and repumping light, and the frequency difference is determined by the hyperfine splitting in

the ground state. Multiple sideband generation should have effects on the interaction between atoms and light. Additional sideband generation will decrease the power of the cooling light and the induced additional excitations would destroy trapped atoms, especially for those having a narrow hyperfine splitting in the ground state like ^{41}K (254 MHz hyperfine splitting).[30] In the experiments for laser cooling of ^{87}Rb with the hyperfine splitting of 6.834 GHz, two-frequency amplification from one single semiconductor TA is a simple and effective way to generate optical pumping and repumping light, without considering the effect of multiple sideband generation due to the large frequency difference of the two-frequency components as discussed above.

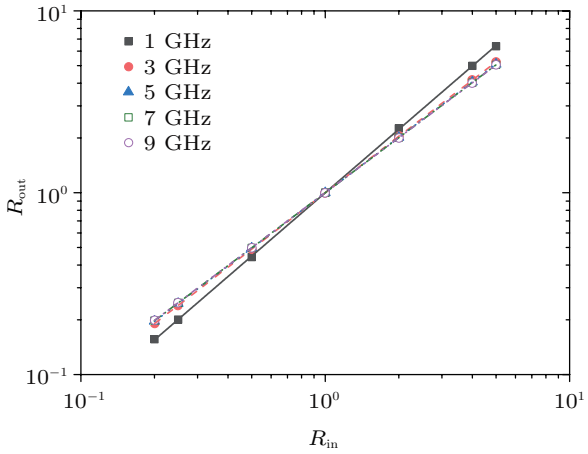


Fig. 5. (color online) TA output power ratio as a function of the input power ratio with a frequency difference of 1 GHz, 3 GHz, 5 GHz, 7 GHz, and 9 GHz. The total injection power is 30 mW.

4. Experimental setup

The experimental setup is shown in Fig. 6. Two external cavity diode lasers (ECDLs) L1 and L2 (DL pro, Toptica, Germany), with a narrow linewidth (1 MHz) and a wide tunability (tens of GHz), are supplied by a current of 220 mA to provide an optical output power of about 80 mW after an integrated optical isolator of 60 dB. The frequency locks are achieved with a feedback via a proportional-integral derivative controller (Digilock110, Toptica) to the diode current and piezoelectric transducers. The frequency ν_1 of the first laser L1 is locked to the atomic transition between $|5^2S_{1/2}, F = 1\rangle$ and $|5^2P_{3/2}, F' = 2\rangle$ states of ^{87}Rb (D2 Line) using a saturated absorption spectroscopy technique.[33] The frequency ν_2 of the second laser L2 is locked to a frequency of 30 MHz red detuned from the atomic transition between $|5^2S_{1/2}, F = 2\rangle$ and $|5^2P_{3/2}, F' = 2\rangle$ states of ^{87}Rb (D2 Line) using an acousto-optic modulation transfer spectroscopy technique.[34] The two lasers have a frequency difference of 6.588 GHz, without further phase locking in our experiments. The output beams of L1 and L2 are combined together in a polarization beam splitter (PBS), i.e., PBS3 in the figure, and coupled into a polarization-maintaining (PM) optical fiber with the same linear polarization. Output signals of the optical fiber are injected into a semiconductor TA (Boost-TA, Toptica, Germany) via optical path 2 for the two-frequency amplification. The TA has a maximum output power of 1.5 W after an integrated optical isolator of 60 dB when pumped by a current of 2150 mA. The TA output beam is divided into two beams after PBS5 for optical spectrum analysis with a home-built FPI (the free spectral range is 1 GHz) and for cold atom experiments, respectively. PBS1, PBS2, and PBS4 along with their corresponding half-wave plates enable the adjustment of the total power and the power ratio between the two lasers at the input of the TA. The output of optical fiber is switched to the optical path 1 for calibrating the FPI or optical spectrum analysis of the input beams. The TA characteristic curve is measured with an optical power meter when the laser of L2 is blocked.

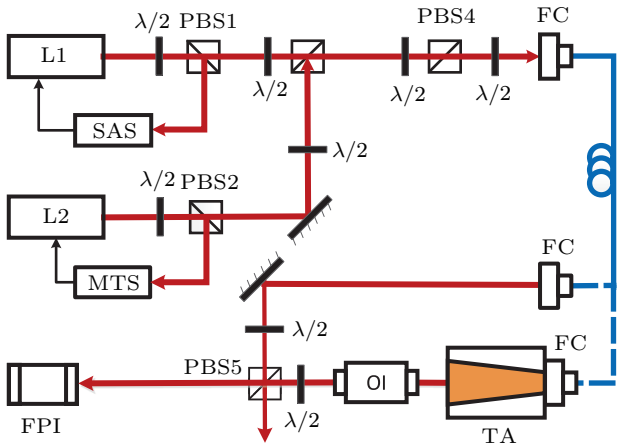


Fig. 6. (color online) Experimental setup. L, diode laser; MTS, modulation transfer spectroscopy; SAS, saturated absorption spectroscopy; $\lambda/2$, half-wave plate; PBS, polarization beam splitter; FC, fiber coupler; TA, tapered amplifier; OI, optical isolator; FPI, Fabry–Perot interferometer.

5. Experimental results

Figure 7 shows the TA output power for different input powers with only L1 as the seeding laser. Each data point in the figure is the average of 100 records of the power meter. The curve fitting is done based on the theoretical model given by Eqs. (4) and (5), and the least squares method is implemented for estimating parameters of the TA. The fitted lines are shown in the figure, and the corresponding values for the parameters of the small signal gain g_0 and amplifier saturation energy E_{sat} are listed in Table 1. Lower input power is required for the TA to run in a saturated gain regime, as the working current is smaller. In a normal operation, 30 mW of the input power are injected into the TA, which operates in the saturated gain regime with the current of 2100 mA at room temperature. It can be observed from Fig. 7 that deviations of the experimental data from the fit data are relatively large when the TA is operated in large working currents. The deviation mainly comes from the measurement error for the TA

output power. One is caused by the failure to accurately measure the TA output power when operating the TA in the range of lower injection laser power, i.e. the less saturated regime. In this regime, the TA output power partly comes from the residual fluorescence of the TA, which reaches the maximum at zero injection laser power. However, we theoretically assume that the TA output power is zero when the injection laser power is zero. It is difficult to remove this measurement error due to the nonlinear decrease of the residual fluorescence with the increased injection laser power. Another important source of measurement error is the failure to accurately measure the saturated output power, which determines the amplifier saturation energy, $E_{\rm sat}$, especially when operating the TA at a large working current. When the TA parameters are estimated via the least squares method, the overestimated output power at lower injection laser power will lead to the positive deviation of the fit data from the experimental data.

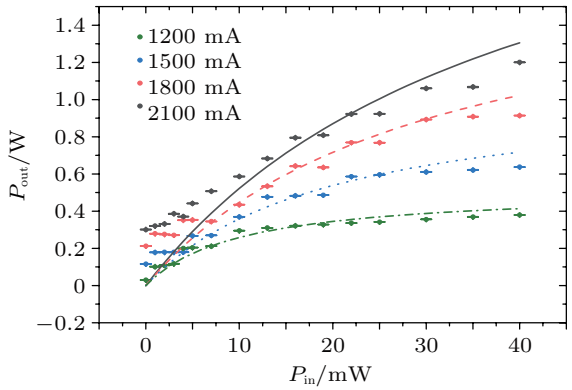


Fig. 7. (color online) TA output power as a function of the input power with a working current of 1200 mA, 1500 mA, 1800 mA, and 2100 mA. Each data point is the average of 100 records of the power meter.

Table 1. TA physical parameters from data fitting.

Current/mA	g_0/m^{-1}	$E_{\rm sat}$/pJ
1200	18804	3
1500	19551	6
1800	21704	9
2100	23731	12

For two-frequency amplification in the TA seeded by lasers of L1 and L2 with a large frequency difference of 6.588 GHz, additional sidebands are negligibly small, as discussed above. In our experiment, we are concerned mainly with the relationship between the TA output power ratio and the input power ratio of two frequency components. Although heterodyne frequency-beat measurement is an efficient method for analyzing the sideband generation and measuring the power ratio,[28–30] especially in the case of the small frequency difference where the FPI cannot distinguish different components due to its limited resolution, it would complicate the optical system with the requirement of an additional reference beam. In contrast, the FPI approach is simple and fast for the potential active power ratio stabilization in the two-frequency amplification scheme, and the resolution is high enough to distinguish the laser frequency difference of 6.588 GHz concerned here, and the accuracy is high enough for measuring the power ratio benefitting from the differential measurement. Therefore, we have adopted the FPI here.

We first calibrate the FPI for measuring the power ratio of the two lasers by the power meter. Two beams from L1 and L2 are coupled into a PM fiber with cross polarizations and pass the FPI. The absolute powers of two beams, measured with the power meter before the FPI, gives the power ratio of the two lasers. In addition, the power ratio can also be inferred from the FPI spectral signals. We recorded 5 FPI spectra for each data point in Fig. 8, and the linear fitting result with a slope of 1.00 ± 0.01 is very close to the expected value of 1, where the measurement uncertainty of 1% may be induced by the power instability of the ECDLs. The calibration result shows that the power ratio can be measured with a relative precision of 1% by the FPI. Note that it is comparable with that by the beat note method (1.4%).[30]

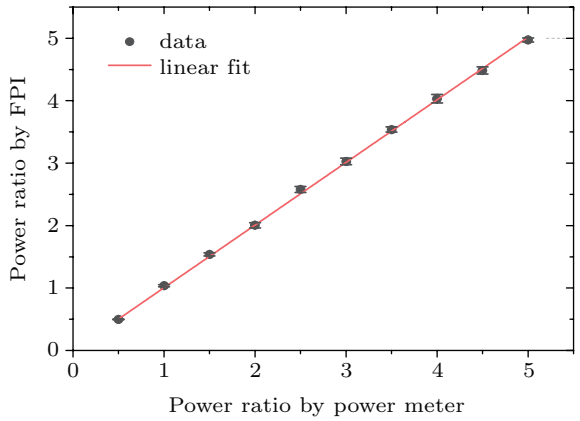


Fig. 8. (color online) Calibration of the power ratio measurement by the FPI.

Figure 9 shows the TA output power ratio versus the input power ratio, with a frequency difference of 6.588 GHz. The TA parameters are fitted with the experimental data

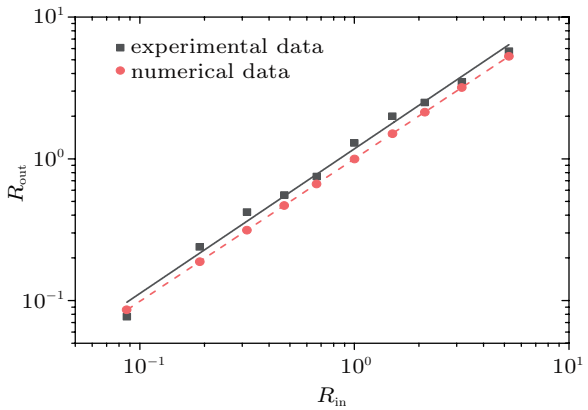


Fig. 9. (color online) The TA output power ratio versus the input power ratio, with a frequency difference of 6.588 GHz. Experimental data (black squares), calculated data (red dots), and the corresponding linear fitting (black solid line and red dashed line, respectively) agree well with each other.

shown in Fig. 7 with the assumption of $g_0 = 23731$ m^{-1} and $E_{\rm sat} = 12$ pJ. In the log–log coordinates, the slopes of the linear fits of the experimental data and the numerical data are 1.01 and 1.02, respectively, which agree very well with each other.

In an atom interferometer, two-frequency amplification injected by the output of two phase-locked ECDLs or an electro-optical phase modulator can be used to generate Raman beams for the coherent manipulation of atomic wavepackets. The intensity ratio I_2/I_1 between two Raman laser beams needs to be adjusted to certain value for eliminating the relative ac Stark shift. This condition is fulfilled for ^{87}Rb atoms[35] considering the $5^2P_{3/2}$ hyperfine splitting, when

$$\frac{I_2}{I_1} = \frac{\left(\frac{1}{60(\Delta+\omega_{\rm eg})} + \frac{1}{4(\Delta-\Delta_2+\omega_{\rm eg})} + \frac{2}{5(\Delta-\Delta_3+\omega_{\rm eg})}\right) - \left(\frac{5}{12\Delta} + \frac{1}{4(\Delta-\Delta_2)}\right)}{\left(\frac{5}{12(\Delta-\omega_{\rm eg})} + \frac{1}{4(\Delta-\Delta_2-\omega_{\rm eg})}\right) - \left(\frac{1}{60\Delta} + \frac{1}{4(\Delta-\Delta_2)} + \frac{2}{5(\Delta-\Delta_3)}\right)}, \tag{11}$$

where Δ stands for the two-photon detuning with respect to $|5^2P_{3/2}, F' = 1\rangle$, Δ_2 and Δ_3 for the energy differences of $|5^2P_{3/2}, F' = 2\rangle$ and $|5^2P_{3/2}, F' = 3\rangle$ with respect to $|5^2P_{3/2}, F' = 1\rangle$, respectively, and $\omega_{\rm eg}$ for the hyperfine splitting of the ground state of $|5^2P_{1/2}, F = 1\rangle$ and $|5^2P_{1/2}, F = 2\rangle$. Equation (11) means that the system is immune to small intensity fluctuations, provided that the ratio of I_2/I_1 remains constant. However, a deviation of this ratio would lead to a decrease in the accuracy of a three-pulse Raman type atom interferometer, due to a non-zero ac Stark shift induced phase error $\Delta\Phi_{\rm ac}$ derived as

$$\Delta\Phi_{\rm ac} = -\frac{2\pi}{\Omega_{\rm eff}}\beta\left(\delta I_2 - k_0\delta I_1\right)16\frac{k_{\rm B}T_{\rm at}}{m}\frac{T(T+t)}{\sigma_0^2}, \tag{12}$$

with $k_0 = I_2/I_1$ chosen to comply with Eq. (11), intensity deviations δI_1, δI_2, Boltzmann constant $k_{\rm B}$, atomic temperature $T_{\rm at}$, Raman laser beam waist σ_0, coefficient $\beta = -3.34$ kHz·mW^{-1}·cm^{-2}, and t being the time between the release of the atoms from the trap and the first Raman pulse. $\Omega_{\rm eff}$ is the effective two-photon Rabi frequency

$$|\Omega_{\rm eff}| = \frac{\Gamma^2\sqrt{k_0}}{4I_{\rm sat}(1+k_0)}\frac{(I_1+I_2)}{\Delta}, \tag{13}$$

with the optical transition linewidth Γ and the saturation intensity $I_{\rm sat}$ ($\Gamma = 2\pi\times 6.07$ MHz and $I_{\rm sat} = 1.67$ mW/cm^2 for ^{87}Rb atoms). Combining Eqs. (12) and (13), the phase error induced by the non-zero ac Stark shift can be deduced as a function of the fluctuation of power ratio δk_0 as

$$\Delta\Phi_{\rm ac} = -\frac{8\pi\beta I_{\rm sat}\Delta}{\Gamma^2}\frac{\delta k_0}{\sqrt{k_0}}16\frac{k_{\rm B}T_{\rm at}}{m}\frac{T(T+t)}{\sigma_0^2}. \tag{14}$$

The intensity ratio of the Raman beams is set simply as k_0, which is about 1.7 with respect to $\Delta = -0.9$ GHz for our experiment of a cold atomic beam interferometer.[36] Considering a cold atomic beam interferometer with the atomic velocity of $v = 10$ m/s, atomic transverse temperature of 146 μK (Doppler limit for laser cooling ^{87}Rb atoms), Raman laser beam waist of 12 mm , $t = 10$ ms, and pulse separation of $L = 100$ mm ($T = 10$ ms), we can calculate the ac Stark shift induced phase error to be -0.35 mrad when $\delta k_0/k_0 = 1\%$. The resulting systematic error is about -0.002 °/h for a cold atomic beam interferometer gyroscope, according to the relation $\delta\Omega = \delta\Phi/(2k_{\rm eff}vT^2)$, where $k_{\rm eff} \sim 1.6\times 10^7$ m^{-1} is the effective wave number of the Raman lasers. This error is about two orders of magnitude higher than the current accuracy (∼68 μdeg/h) of the best atom gyroscope, but can be further reduced by reversing the sign of the effective Raman propagation vector.[18] If the atomic transverse temperature can be cooled further to 3 μK, the resulting systematic error is about -7.3 μrad and the gyroscope systematic error is about -47 μdeg/h. Equation (14) shows that the ac Stark shift related phase error is determined by the fluctuation of the power ratio and independent of that of the absolute laser power. Therefore, active strategy for stabilizing the power ratio is necessary for building a high precision atom interferometer gyroscope. Our experimental result demonstrates that the real-time measurement of the power ratio with the resolution of 1% can be implemented in a FPI method.

6. Conclusions

Two-frequency amplification in a semiconductor TA has been investigated numerically and experimentally in this paper. We used a finite-difference method based on a simplified model to numerically simulate the output of the TA when injected by two CW lasers. The effect of multiple sideband generation was investigated by homodyne frequency-beat signals, concerned with the influences of frequency difference, injection laser power, and power ratio of the two-frequency components. The numerical result shows that multiple sideband generation can be neglected when the frequency difference is large enough (> 2 GHz). It also shows that the TA tends to linearly amplify the power ratio between the two-frequency seeding components with the increase of the frequency difference.

We also investigated the power ratio relationship between the output and input of the TA experimentally with a frequency difference of 6.588 GHz, based on a calibrated FPI measurement. The measurement shows a relative precision of 1%, limited by the accuracy of the power meter. This agrees well with the numerical result based on the fitting of the experimental data. In the numerical simulation and experiment, we did not consider the influence of the relative phase fluctuation of two injection lasers on the output power ratio. This can be neglected when the frequency difference of two injection lasers is large and only the power ratio relationship between the output and input of the TA is concerned. Quantitative analysis and measurement for the influence of the coherence and relative phase noise of two injection lasers on the two-frequency amplification process need be done in the future.

The scheme of two frequency amplification by a semiconductor TA is now being applied in our experiments of an atomic interferometer to generate high power two-frequency laser source for optical pumping and repumping in laser cooling of atoms, and Raman beams via an electro-optical phase modulator for coherent manipulation of atom wave-packet. Both cases require accurate control on the power ratio of two frequency laser components. An active stabilization strategy based on the FPI measurement of the power ratio can be used for locking the power ratio of two frequency components and improving the long-term stability of an atom interferometer based sensor.

Acknowledgment

The authors thank Chi Xu and Lijun Wang for helpful discussion.

References

[1] Chi M, Jensen O B and Petersen P M 2011 *Opt. Lett.* **36** 2626
[2] Liu W X and Sun M Z 2016 *Chin. Phys. Lett.* **33** 024206
[3] Süptitz W, Wokurka G, Strauch F, Kohns P and Ertmer W 1994 *Opt. Lett.* **19** 1571
[4] Bloch I, Greiner M, Mandel O, Hänsch T W and Esslinger T 2001 *Phys. Rev. A* **64** 021402
[5] Modugno G, Ferrari G, Roati G, Brecha R J, Simoni A and Inguscio M 2001 *Science* **294** 1320
[6] Tien T Q, Maiwald M, Sumpf B, Erbert G and Tränkle G 2008 *Opt. Lett.* **33** 2692
[7] Zhang Y G, Zhang H, Dou G and Xu J G 2017 *Acta Phys. Sin.* **66** 233101 (in Chinese)
[8] Zhang S, Wu W, Wu C W, Li F G, Li T, Wang X and Bao W S 2017 *Chin. Phys. B* **26** 074205
[9] Guo W X and Liu W M 2016 *Physics* **45** 370
[10] Kasevich M and Chu S 1991 *Phys. Rev. Lett.* **67** 181
[11] Wynands R and Nagel A 1999 *Appl. Phys. B* **68** 1
[12] Holzwarth R, Udem Th Hänsch T W, Knight J C, Wadsworth W J and Russell P St J 2000 *Phys. Rev. Lett.* **85** 2264
[13] Cruz F C, Stowe M C and Ye J 2006 *Opt. Lett.* **31** 1337
[14] Guan H, Huang Y, Liu P L, Bian W, Shao H and Gao K L 2015 *Chin. Phys. B* **24** 054213
[15] Gustavson T L, Landragin A and Kasevich M A 2000 *Classical Quantum Gravity* **17** 2385
[16] Peters A, Chung K Y and Chu S 2001 *Metrologia* **38** 25
[17] McGuirk J M, Foster G T, Fixler J B, Snadden M J and Kasevich M A 2002 *Phys. Rev. A* **65** 033608
[18] Durfee D S, Shaham Y K and Kasevich M A 2006 *Phys. Rev. Lett.* **97** 240801
[19] Canuel B, Leduc F, Holleville D, Gauguet A, Fils J, Virdis A, Clairon A, Dimarcq N, Bordé C J and Landragin A 2006 *Phys. Rev. Lett.* **97** 010402
[20] Louchet-Chauvet A, Farah T, Bodart Q, Clairon A , Landragin A, Merlet S and Santos F P D 2011 *New J. Phys.* **13** 065025
[21] Xue H B, Feng Y Y, Wang X J, Chen S and Zhou Z Y 2013 *Rev. Sci. Instrum.* **84** 046104
[22] Sorrentino F, Bodart Q, Cacciapuoti L, Lien Y H, Prevedelli M, Rosi G, Salvi L and Tino G M 2014 *Phys. Rev. A* **89** 023607
[23] Gillot P, Francis O, Landragin A, Santos F, Pereira D and Merlet S 2014 *Metrologia* **51** L15
[24] Dutta I, Savoie D, Fang B, Venon B, Garrido Alzar C L, Geiger R and Landragin A 2016 *Phys. Rev. Lett.* **116** 183003
[25] Wu X J, Zi F, Dudley J, Bilotta R J, Canoza P and Müller H 2017 *Optica* **4** 1545
[26] Agrawal G P and Olsson N A 1989 *IEEE J. Quantum Electron.* **25** 2297
[27] Ferrari G, Mewes M, Schreck F and Salomon C 1999 *Opt. Lett.* **24** 151
[28] Luo H, Li K, Zhang D F, Gao T Y and Jiang K J 2013 *Opt. Lett.* **38** 1161
[29] Lévèque T, Gauguet A, Chaibi W and Landragin A 2010 *Appl. Phys. B* **101** 723
[30] Zhan S, Duan X C, Zhou M K, Yao H B, Xu W J and Hu Z K 2015 *Opt. Lett.* **40** 29
[31] Cheng B, Gillot P, Merlet S and Pereira Dos Santos F 2015 *Phys. Rev. A* **92** 063617
[32] Hill M T, Tangdiongga E, de Waardt H, Khoe G D and Dorren H J S 2002 *Opt. Lett.* **27** 1625
[33] Siddons P, Adams C S, Ge C and Hughes I G 2008 *J. Phys. B: At. Mol. Opt. Phys.* **41** 155004
[34] Zhang J, Wei D, Xie C and Peng K 2013 *Opt. Express* **11** 1338
[35] Schmidt M 2011 *A Mobile High-precision Gravimeter Based on Atom Interferometry* (Ph.D. Dissertation) (Berlin: Humboldt-University)
[36] Xue H B, Feng Y Y, Chen S, Wang X J, Yan X S, Jiang Z K and Zhou Z Y 2015 *J. Appl. Phys.* **117** 094901